

飞秒激光刻写光纤光栅实现 9 kW 全光纤振荡器

李昊^{1,2}, 杨保来^{1,2}, 饶斌裕^{1,2}, 叶新宇^{1,2}, 田鑫^{1,2}, 王蒙^{1,2}, 武柏屹^{1,2}, 赵蓉^{1,2}, 李智贤^{1,2}, 陈子伦^{1,2},
肖虎^{1,2}, 马鹏飞^{1,2}, 王泽锋^{1,2*}, 陈金宝^{1,2}

¹国防科技大学前沿交叉学科学院, 湖南 长沙 410073;

²国防科技大学南湖之光实验室, 湖南 长沙 410073

摘要 光纤光栅(FBG)在高功率光纤振荡器中发挥着重要作用,既可以作为谐振腔腔镜,又可以抑制受激拉曼散射(SRS)效应。使用飞秒激光在芯径为 30 μm 的大模场双包层光纤(LMA-DCF)上刻写了波长为 1080 nm 的 FBG 对以及波长为 1135 nm 的啁啾倾斜光纤光栅(CTFBG),利用 FBG 对搭建了全光纤振荡器,并使用 CTFBG 抑制了 SRS,实现了 9 kW 激光功率输出,斜率效率为 83.4%。研究结果有利于推动高功率 FBG 的研制和高功率光纤振荡器的发展。

关键词 光纤光学; 飞秒激光; 光纤振荡器; 高功率激光器; 受激拉曼散射; 光纤光栅

中图分类号 TN248

文献标志码 A

DOI: 10.3788/CJL231429

高功率光纤振荡器在高端制造等领域中有着广泛的应用^[1]。近年来,光纤振荡器的输出功率不断突破。2020年,日本藤仓公司报道了 8 kW 的全光纤振荡器^[2];2023年,国防科技大学也报道了 8 kW 级的全光纤振荡器^[3]。光纤光栅(FBG)是高功率光纤振荡器中的核心器件。一方面,FBG 作为振荡器的谐振腔腔镜,起到选择波长和耦合输出功率的作用。另一方面,特殊设计的 FBG,例如啁啾倾斜光纤光栅(CTFBG)^[4-6],可以作为拉曼光滤除器,抑制振荡器中的受激拉曼散射(SRS)效应。这两类高功率 FBG 的传统制备方法为紫外曝光法,在刻写 FBG 前需要对光纤进行载氢处理以增加光敏性,在刻写 FBG 后需要通过热退火消除残余的氢分子与刻写过程中生成的羟基。当退火不彻底时,FBG 中残余的氢气与羟基会吸收激光并发热,成为限制其承受功率的主要因素。目前紫外曝光法刻写的腔镜用 FBG 与 CTFBG 的最高承受功率分别为 8 kW^[2]与 4.3 kW^[7]。使用飞秒激光刻写高功率 FBG 可以有效解决氢气和羟基引起的 FBG 发热问题。因为飞秒激光可以直接在光纤中刻写 FBG,光纤不需要载氢增敏处理。目前,飞秒激光刻写的 CTFBG 的承受功率已突破 10 kW,但是利用飞秒激光刻写的腔镜用 FBG 只实现了 8 kW 的全光纤振荡器^[3],振荡器功率的提升受限于模式不稳定(TMI)效应。近期,国防科技大学南湖之光实验室采用飞秒

激光相位掩模板法在大模场双包层光纤(LMA-DCF)上刻写了中心波长为 1080 nm 的高反(HR)与低反(LR) FBG,用于搭建全光纤振荡器。通过在 LR FBG 的一侧刻写 CTFBG,抑制 SRS 效应并提高 TMI 阈值,振荡器的输出功率被提升至 9050 W。

实验采用与文献[3,8]相同的系统刻写腔镜用 FBG 与 CTFBG,刻写前须剥除光纤涂覆层。在一根纤芯/包层直径为 30 μm /600 μm 的 LMA-DCF 上刻写了 HR FBG,在一根纤芯/包层直径为 30 μm /250 μm 的 LMA-DCF 上刻写了 LR FBG。图 1(a)展示了 HR FBG 和 LR FBG 的反射谱,其中心波长为 1080 nm。HR FBG 和 LR FBG 的 3 dB 带宽分别为 4.0 nm 和 2.1 nm,前者反射率大于 99%,后者的反射率约为 6%,适当降低 LR FBG 的反射率有助于提高振荡器的效率。将 CTFBG 与 LR FBG 刻写在同一根光纤上,使振荡器系统更加紧凑稳定,CTFBG 的光谱如图 1(b)所示。透射谱的中心波长为 1135 nm,3 dB 带宽约为 18 nm,最大深度为 15 dB。图 2 展示了光纤振荡器的结构示意图。振荡器采用纯后向泵浦方案,增益光纤是长度为 38 m、纤芯/包层直径为 30 μm /600 μm 的掺镱光纤(YDF)。使用 969 nm+982 nm 双波长半导体激光器(LD)作为泵浦源,可以减小 YDF 单位长度的热负载,从而提高 TMI 阈值^[9-10]。使用一个泵浦/信号合束器耦合泵浦光,其信号输入/输出光纤的纤芯/包层直径

收稿日期: 2023-11-23; 修回日期: 2023-12-11; 录用日期: 2023-12-20; 网络首发日期: 2023-12-28

基金项目: 国家自然科学基金(11974427, 12004431, 62005315)、湖南省科技创新计划项目(2021RC4027)、脉冲功率激光技术国家重点实验室主任基金(SKL2020ZR05, SKL2021ZR01)

通信作者: *zefengwang_nudt@163.com

分别为 $30\ \mu\text{m}/600\ \mu\text{m}$ 和 $30\ \mu\text{m}/250\ \mu\text{m}$ 。图 2 虚线框所示为 CTFBG, 其被刻写在 LR FBG 的一侧且位于谐振腔内, 用于抑制 SRS 效应。除了引入一个 CTFBG, 振荡器系统的其他部分不作改变。此外, 为

了提升振荡器的输出功率, 其输出端未加入包层光滤除器 (CLS)。这是因为出现 TMI 效应后, 从纤芯处泄漏到包层的信号光增多, 包层光被 CLS 滤除会使得振荡器效率下降。

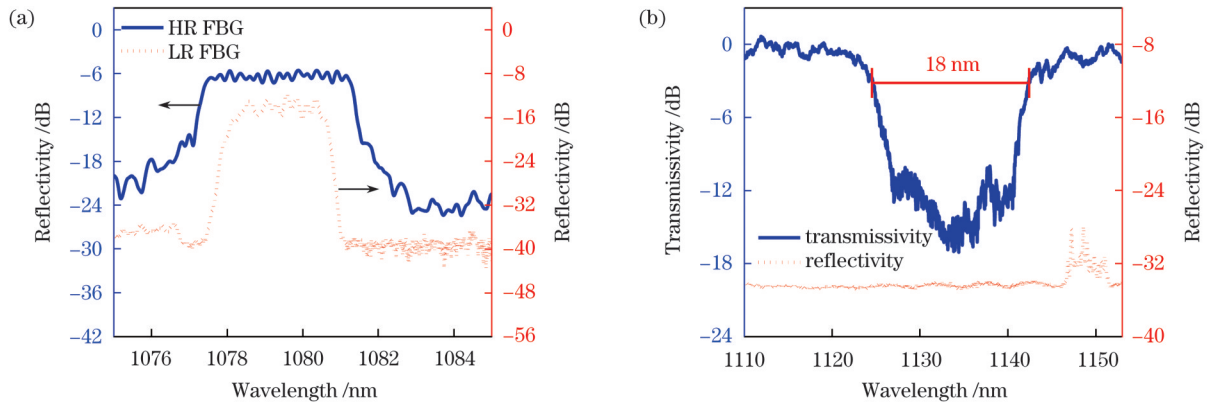


图 1 FBGs 的测量光谱。(a) HR FBG 和 LR FBG; (b) CTFBG
Fig. 1 Measured spectra of FBGs. (a) HR FBG and LR FBG; (b) CTFBG

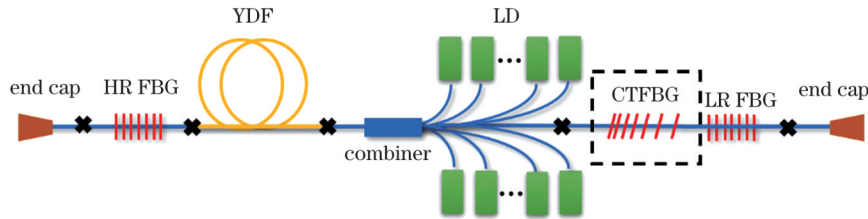


图 2 光纤振荡器的结构示意图
Fig. 2 Structural diagram of fiber oscillator

实验结果如图 3 所示。图 3(a) 展示了刻写 CTFBG 前后最高功率下的输出光谱。由于 SRS 被 CTFBG 有效抑制, 1135 nm 波长的拉曼光的强度下降 16 dB, 且光谱展宽现象也得到抑制。图 3(b) 展示了刻写 CTFBG 前后输出时序信号对应的频谱。未出现 TMI 现象时, 频谱中只在 12 kHz 处有一个基底频率噪声引起的频率峰。当输出功率增大到 8250 W 时, 在 20 kHz 处出现了一个新的频率峰, 意味着出现了 TMI 现象。在刻写 CTFBG 后, 当输出功率增大到 8700 W 时, 才在 4 kHz 处出现新的频率峰, 所以 TMI 阈值从 8250 W 提高至 8700 W。这是因为 SRS 也会

诱导 TMI 的产生, 所以当 SRS 被抑制时, TMI 阈值也会有所提高^[11]。图 3(c) 展示了插入 CTFBG 前后的输出功率变化。在刻写 CTFBG 后, 斜率效率由 85.4% 下降到 83.4%, CTFBG 的插损约为 2%。尽管斜率效率下降, 但是由于 SRS 被抑制以及 TMI 阈值的提升, 输出功率由 8910 W 提高至 9050 W, 功率的进一步提升受限于 TMI。实验中, 使用带水冷散热系统的金属热沉, 通过填充高效导热硅脂, 对 HR FBG、LR FBG 和 CTFBG 进行散热处理, 光栅在最高功率下的温度均小于 $40\ ^\circ\text{C}$, 具有承受更高功率的潜力。

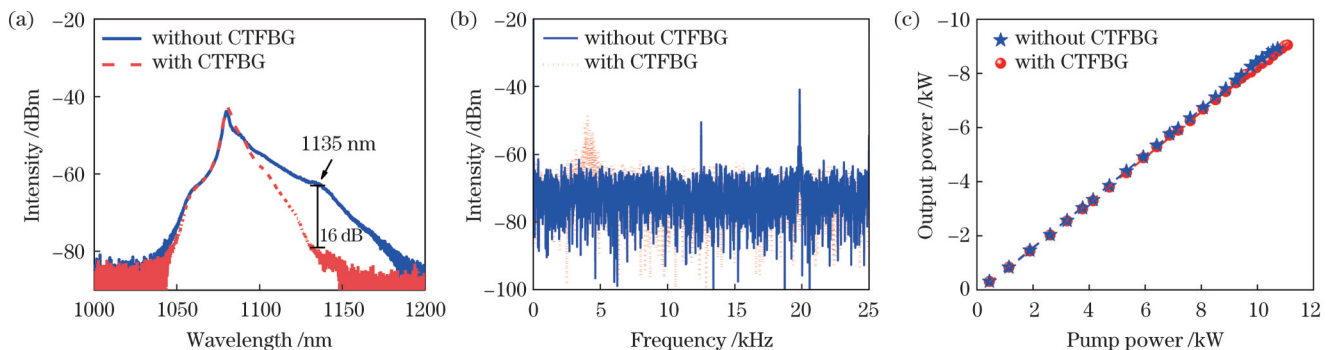


图 3 测试结果。(a) 输出光谱; (b) 输出时序信号对应的频谱; (c) 输出功率
Fig. 3 Test results. (a) Output spectra; (b) frequency spectra corresponding to output time-domain signals; (c) output power

本文基于飞秒激光刻写 FBG 对搭建了全光纤振荡器, 并通过飞秒激光刻写 CTFBG 抑制了 SRS, 进而提高了 TMI 阈值, 最终实现了 9 kW 激光功率输出。今后将通过进一步抑制 TMI, 实现基于飞秒激光刻写 FBG 的 10 kW 全光纤振荡器。

参 考 文 献

- [1] 王小林, 张汉伟, 杨保来, 等. 高功率掺镱光纤振荡器: 研究现状与发展趋势[J]. 中国激光, 2021, 48(4): 0401004.
Wang X L, Zhang H W, Yang B L, et al. High-power ytterbium-doped fiber laser oscillator: current situation and future developments[J]. Chinese Journal of Lasers, 2021, 48(4): 0401004.
- [2] Wang Y, Kitahara R, Kiyoyama W, et al. 8-kW single-stage all-fiber Yb-doped fiber laser with a BPP of 0.50 mm-mrad[J]. Proceedings of SPIE, 2020, 11260: 1126022.
- [3] Li H, Yang B L, Wang M, et al. Femtosecond laser fabrication of large-core fiber Bragg gratings for high-power fiber oscillators[J]. APL Photonics, 2023, 8(4): 046101.
- [4] Jiao K R, Shu J, Shen H, et al. Fabrication of kW-level chirped and tilted fiber Bragg gratings and filtering of stimulated Raman scattering in high-power CW oscillators[J]. High Power Laser Science and Engineering, 2019, 7: e31.
- [5] Song H Q, Yan D L, Wu W J, et al. SRS suppression in multi-kW fiber lasers with a multiplexed CTFBG[J]. Optics Express, 2021, 29(13): 20535-20544.
- [6] 李昊, 叶新宇, 王蒙, 等. 基于飞秒激光刻写的高功率啁啾倾斜光纤光栅[J]. 光学学报, 2023, 43(17): 1706002.
Li H, Ye X Y, Wang M, et al. High-power chirped and tilted fiber gratings written by femtosecond lasers[J]. Acta Optica Sinica, 2023, 43(17): 1706002.
- [7] 王蒙, 田鑫, 赵晓帆, 等. 国产 25 $\mu\text{m}/400 \mu\text{m}$ 啁啾倾斜光纤光栅传输功率突破 4 kW[J]. 中国激光, 2022, 49(6): 0615001.
Wang M, Tian X, Zhao X F, et al. Transmission power of homemade chirped and tilted fiber Bragg grating on 25 $\mu\text{m}/400 \mu\text{m}$ fiber exceeding 4 kW[J]. Chinese Journal of Lasers, 2022, 49(6): 0615001.
- [8] Li H, Wang M, Wu B, et al. Femtosecond laser fabrication of chirped and tilted fiber Bragg gratings for stimulated Raman scattering suppression in kilowatt-level fiber lasers[J]. Optics Express, 2023, 31(8): 13393-13401.
- [9] Wan Y C, Xi X M, Yang B L, et al. Enhancement of TMI threshold in Yb-doped fiber laser by optimizing pump wavelength[J]. IEEE Photonics Technology Letters, 2021, 33(13): 656-659.
- [10] Wan Y C, Yang B L, Wang P, et al. Optimizing the pump wavelength to improve the transverse mode instability threshold of fiber laser by 3.45 times[J]. Journal of Modern Optics, 2021, 68(18): 967-974.
- [11] Hejaz K, Shayganmanesh M, Rezaei-Nasirabad R, et al. Modal instability induced by stimulated Raman scattering in high-power Yb-doped fiber amplifiers[J]. Optics Letters, 2017, 42(24): 5274-5277.

9 kW All-Fiber Oscillator Based on Fiber Gratings Inscribed by Femtosecond Lasers

Li Hao^{1,2}, Yang Baolai^{1,2}, Rao Binyu^{1,2}, Ye Xinyu^{1,2}, Tian Xin^{1,2}, Wang Meng^{1,2}, Wu Baiyi^{1,2}, Zhao Rong^{1,2}, Li Zhixian^{1,2}, Chen Zilun^{1,2}, Xiao Hu^{1,2}, Ma Pengfei^{1,2*}, Wang Zefeng^{1,2*}, Chen Jinbao^{1,2}

¹College of Advanced Interdisciplinary Studies, National University of Defense Technology, Changsha 410073, Hunan, China;

²Nanhu Laser Laboratory, National University of Defense Technology, Changsha 410073, Hunan, China

Abstract

Objective High-power fiber oscillators have significant applications in industrial processing and other fields. Fiber Bragg gratings (FBGs) are key components of high-power fiber oscillators. On the one hand, FBGs can act as cavity mirrors of high-power fiber oscillators to select a signal wavelength and couple output signal power. On the other hand, FBGs with special designs such as chirped and tilted fiber Bragg gratings (CTFBGs) can be used to suppress stimulated Raman scattering (SRS) in high-power fiber oscillators. Generally, the traditional approach for fabricating these two types of FBGs is the ultraviolet laser (UV) phase-mask method. However, hydrogen-loaded and thermally annealed treatments are required. When annealing is not thorough, the residual hydrogen and hydroxyl groups in the FBGs will absorb lasers to generate heat, which is the main factor limiting the power FBGs can withstand. To date, the maximum handling powers of mirror FBGs and CTFBGs written using UV lasers are 8.0 kW and 4.3 kW, respectively. The development of femtosecond laser inscription technology provides a promising new method for the inscription of FBGs. FBGs can be directly inscribed into fibers without hydrogen loading. Thus, the heating generated by the hydrogen and hydroxyl groups in FBGs can be avoided. Currently, the handling power of a CTFBG written using femtosecond lasers exceeds 10 kW. However, the maximum output power of the all-fiber oscillator based on femtosecond-laser-written FBGs is 8 kW due to the limitations of transverse mode instability (TMI).

Methods FBGs and CTFBGs used in cavity mirrors are written using the femtosecond-laser phase-mask method. Figure 1(a) shows the reflection spectra of the high-reflectivity FBG (HR FBG) and low-reflectivity FBG (LR FBG). The 3-dB bandwidths of the HR FBG and LR FBG are 4.0 nm and 2.1 nm with reflectivities of more than 99% and approximately 6%, respectively. Figure 1(b) shows the CTFBG spectrum. The central wavelength of the transmission spectrum is 1135 nm with a 3-dB bandwidth of approximately 18 nm and maximum depth of 15 dB. Figure 2 shows the setup of the fiber oscillator. The oscillator employs a counter-

pumping scheme with an active $30\ \mu\text{m}/600\ \mu\text{m}$ ytterbium-doped fiber (YDF) and pump source of $969\ \text{nm}+982\ \text{nm}$ dual-wavelength diode laser (LD). The dashed box in Fig. 2 indicates the CTFBG, which is inscribed on the side of the LR FBG and located in the resonator to ensure the oscillator system is compact and stable.

Results and Discussions Figure 3(a) shows the output spectra at maximum output powers. Due to the suppression of SRS by the CTFBG, the Raman light intensity at $1135\ \text{nm}$ decreases by approximately $16\ \text{dB}$. In addition, the TMI threshold of the oscillator increases from $8250\ \text{W}$ to $8700\ \text{W}$ with the CTFBG, as shown in Fig. 3(b). Figure 3(c) shows the changes in the output power. The slope efficiency decreases from 85.4% to 83.4% with the CTFBG. Therefore, the insertion loss of the CTFBG is approximately 2% . Despite the decrease in slope efficiency, the output power increases from $8910\ \text{W}$ to $9050\ \text{W}$ due to the suppression of the SRS and the increase in the TMI threshold.

Conclusions This study demonstrates an all-fiber oscillator with maximum output power. An all-fiber oscillator is constructed based on femtosecond-laser-written FBGs, and femtosecond-laser-written CTFBGs are used to suppress the SRS, ultimately achieving a 9-kW laser power output.

Key words fiber optics; femtosecond laser; fiber oscillators; high-power lasers; stimulated Raman scattering; fiber gratings